CHAPTER FOUR

Synthesis and applications of Pd-WO_3-SiO_2 nanocomposite

This chapter deals with synthesis and characterization of Pd-WO_3-SiO_2-PB nanocomposite further investigations have been made to verify the quality of present nanocomposite material in the development of electrochemical sensor for hydrogen peroxide and furthermore Intrinsic peroxidise like activity of WO_3, Pd-WO_3-SiO_2 and Pd-WO_3-SiO_2-PB nanocomposite was also explored.

4.1. INTRODUCTION

Nanostructure metal oxides have shown promising applications as an appropriate environment for the immobilization of enzyme at the electrode surface [Chopra, Nitin et al., (2007a); Liu, Aihua, (2008); Valentini and Palleschi, (2008); Varghese and Grimes, (2003)]. Stable immobilization of macromolecular bio-molecules on semiconducting metal oxide nanosurface with complete retention of their biological recognition properties is a crucial problem for the commercial development of miniaturized biosensor. Large specific surface area and high surface free energy of nanoparticles enable strong absorption of enzymes required for efficient designing of electrochemical biosensor [Chopra, Nitin et al., (2007a); Liu, Aihua, (2008); Valentini and Palleschi, (2008)]. Generally, the adsorption of enzymes directly onto naked surfaces of bulk materials may frequently result in their denaturation and loss of bioactivity. However, the adsorption of such enzyme onto the surfaces of nanoparticles can retain their bioactivity because of biocompatible nature of metal oxides nanoparticles [Luo et al., (2006)]. Sol-gel derived nanostructured metal oxides justifying interesting properties; such as better thermal stability, low cost, biocompatibility, non-toxicity and low temperature processing, etc.; have attracted much interest for immobilization of desired bio-molecules [Li, Juan et al., (1996)]. The nanostructured materials such as metals (Au, Pt, Ag, Cu, Rh and Pd) nanoparticles and their composite with metal oxide have been extensively used in bioaffinity sensors[Fritzsche and Taton, (2003); Li, Juan et al., (1996)]. Metal oxide nanoparticles such as tungsten Oxide (WO_3), titanium oxide (TiO_2), zinc oxide (ZnO), cerium oxide (CeO_2), tin oxide (SnO_2), and zirconium oxide (ZrO_2) have been recently used for fabrication of enzyme-based biosensors [Asif et al., (2010); Curulli et al., (2005); Deng, Z. et al., (2009); Feng et al., (2006); Liu, Jinping et al., (2009); Patil, Dewyani et al., (2012a); Zuo, Shao-Hua et al., (2009)]. Furthermore, WO_3 nanoparticle film has been employed as a matrix with cytochrome C (cyt. C), for detection of hydrogen peroxide (H_2O_2), in order to assemble a new generation of chemical sensors and biosensors [Deng, Z. et al., (2009)]. WO_3

nanoparticles have attracted much interest owing to their unique properties of electrochromism, high mechanical strength, oxygen ion conductivity, wide band gap (3.0eV), isoelectric point (~ 0.5), biocompatibility and retention of biological activities and have been used for H_2O_2 sensing [Bigey et al., (1999); Deng, Z. et al., (2009); Feng et al., (2006); Lee, S-H et al., (2006); Lu, Dong Yu et al., (2008)]. The sensitive and selective determination of H_2O_2 has been a challenging requirement because it is not only the byproduct of enzymatic reaction but also effluent of many industrial processes.

The inorganic nonmaterial's so as to enzymes are very interesting as they have better properties comparing to natural enzymes like more resistance to pH, temperature, protease digestion, easier to prepare and store. This intended us to study the following: (1) to understand the biocompatibility of WO_3 for enzyme immobilization and to evaluate its role in biocatalysis, and (2) to evaluate the possibility on the formation of nanocomposite consisting of the matrix material containing the nanosized reinforcement components facilitating the electron transfer and catalytic performances of nanocomposite. In particular, palladium and Prussian blue nanoparticles (PdNPs and PBNPs) based nanocomposites attract special research interest because both components illustrate admirable electrochemical properties for potential applications. In addition to that the intrinsic peroxidase-like activity of nanomaterials directed us to examine similar activity of WO_3 and its nanocomposite. Fortunately, we got interesting finding on these line that led to examine further on the peroxidase mimetic and electrochemical behavior of the nanocomposite toward detection of H_2O_2. We have developed a library of electrocatalytic sites in nanostructured domain for H_2O_2 analysis and the findings revealed that electrocatalysis is greatly amplified as a function of nanogeometery [Pandey and Pandey, (2012); Pandey and Pandey, (2013b);)]. Beside this, we have recently reported the novel synthesis of PBNPs sol and evaluated their role for electrochemical sensing of H_2O_2 [Pandey and Pandey, (2013a)]. We also studied the effect of metal oxide and their Pd nanocomposite in electrochemical sensing of ascorbic acid.

These finding directed us to design the nanocomposite of WO_3 re-enforcing the properties of palladium embedded within silica matrix and PBNPs which led to develop three different systems of nanomaterial designated as (1) WO_3, (2) Pd-WO_3-SiO_2 and (3) Pd-WO_3-SiO_2-PB for evaluating their relative activity in H_2O_2 sensing.

The determination of hydrogen peroxide (H_2O_2) has great interest in many research fields, such as clinical, food, pharmaceutical, and environmental analysis [Chen, Shihong et al., (2013b); Lu, Xingping et al., (2014); Chen, Wei et al., (2012b)]. Beside this, H_2O_2 is the side product of a reaction catalyzed by oxidase enzymes [Ali et al., (2011)]. Therefore, it is of particular importance to determine the concentration of H_2O_2 with high sensitivity, low detection limit, long stability, and good reproducibility. To date, various analytical techniques have been reported for its determination but these techniques are insufficient in sensitivity, specificity, and use of expensive reagents. Electroanalytical methods have gained much attention since they achieve low detection limits and rapid response times. Direct electrochemical reduction and oxidation of H_2O_2 at unmodified electrodes have been limited by the slow kinetics and surface fouling beside this; low sensitivity, poor reproducibility, and low stability are other limitations of using unmodified electrodes for H_2O_2 detection. In order to solve the problems mentioned above, modified electrodes have been used to improve the electrochemical reaction of H_2O_2. The operation mechanism of modified electrodes depends on the properties of the modifier materials used to promote selectivity and sensitivity towards the target species. Among various modifiers reported for electrode modification, metal oxide (MOs) and metal nanoparticle based modifiers have been proved worthy for electroanalytical application and accordingly the present subject matter is of great potentiality in dealing the H_2O_2 analysis. As discussed previously, the PB is recognized for its exciting electrochemical and electrocatalytic properties, and exhibits high activity and selectivity towards H_2O_2 reduction so-called "artificial peroxidase". Therefore, in the present investigation we intended the use of above synthesized WO_3, Pd-WO_3-SiO_2, Pd-WO_3-SiO_2-PB and HRP

coupled Pd-WO_3-SiO_2-PB nanocomposite in H_2O_2 sensing. The results based on cyclic voltammetry, amperometery and chronoamperometry are shown and discussed *vide infra*.

Peroxidase enzyme has been extensively applied in many physiological reactions due to their high efficiency and specificity; however, they bear some intrinsic drawbacks such as low stability due to denaturation and digestion, dependency on environmental condition and expensive preparation as well as purification. These disadvantages have gained the researches attention to fabricate enzyme mimetics. Nanoparticles that mimic enzymes have become popular as they have potentiality for bio-signal amplification, mainly because of their large surface area, high catalytic activity, and low cost. Encouraged by multifunctional applications of inorganic nanomaterials, ongoing efforts are in progress to fabricate enzyme mimetics, which reveal enzyme mimicking property along with stability and robustness to high temperature and pH. Recently, it is reported that many nanomaterials could possess intrinsic peroxidase like activity and have justified their use as peroxidase substitute for health and health care advances [Bhattacharya et al., (2011); Chen, Y. et al., (2013c); Liu, X. et al., (2012); Ma et al., (2012); Malvi et al., (2012); Wang, W. et al., (2012); Wei and Wang, (2013); Yu et al., (2009); Zhang, Y. et al., (2012c); Qiao et al., (2014); Deng, Hao-Hua et al., (2014)]. There is still challenging demand to enhance the catalytic efficiency of such nanomaterials to the equivalent of biocatalytic activity thereby allowing the precise control of the mimetic character and ultimately leading to the development of new materials as powerful peroxidases i.e. Horseradish peroxidase (HRP) replacement during enzyme and immunosensors development. This motivated us to study whether the PBNPs and its mixed metal analogues with verity of transition metal ions like Mn, Ni and Cu efficiently catalyzed the oxidation of typical peroxidase substrates directly or not. Accordingly, the present chapter has been also intended to investigate the performance of peroxidase like behavior of WO_3, Pd-WO_3-SiO_2 and Pd-WO_3-SiO_2-PB nanocomposite based on the catalytic oxidation of o-dianisidine.

4.2. EXPERIMENTAL

4.2.1. Materials

Potassium ferricyanide, cyclohexanone, hydrogen peroxide, phenol and pyrogallol were purchased from Merck, India. Sodium tungustate, cation exchange resin, 3-Glycidoxypropyltrimethoxysilane (GPTMS), graphite (particle size 1-2 μm), Horseradish peroxidase (HRP), palladium chloride, Nujol oil (density 0.838 g/mL), Palladium chloride, o-dianisidine and 3-aminopropyltrimethoxysilane (3-APTMS) were obtained from Sigma-Aldrich Chemical Co., India. Aqueous solutions were prepared by using doubly distilled-deionized water (Alga water purification system). The solutions of H_2O_2 were freshly prepared in double distilled water before each experiment. Unless mentioned otherwise, all the experiments were performed at room temperature.

4.2.2. Preparation of WO_3, Pd-WO_3-SiO_2 and Pd-WO_3-SiO_2-PB nanocomposites

WO_3 nanoparticles were prepared as follows: Protonated cation exchanger resin was packed in glass column. The packed resin was washed with distilled water repeatedly until pH of the effluent came close to 7. The ion-exchange capacity (content of protons) of the resin was about 2 meq./cm^3, as evaluated from the titration with NaOH solution. Aqueous solution of sodium tungstate hydrate ($Na_2WO_4.2H_2O$) was allowed to flow through the glass column at a fixed flow rate followed by collection of transparent sol of tungstic acid into a beaker. After keeping standing for 3 days, the effluent precipitated into a yellow gel containing $WO_3.2H_2O$. The resulting gel was dried at room temperature and calcinated at 450 $^{\circ}$C to obtain WO_3 nanoparticle powder as reported earlier [Choi, Yong-Gyu et al., (2002)].

Pd-WO_3-SiO_2 nanocomposite was made from the effluent sol of WO_3 mixed with palladium (Pd) linked 3-glycidoxypropyltrimethoxysilane having Pd:W ratio to the order of (5%) and allowed to sonicate for 20 min. Palladium linked 3-glycidoxypropyltrimethoxysilane was made by adding 50 μL aqueous

solution of palladium chloride (1 mg/mL) in 100 µL of 3-glycidoxypropyltrimethoxysilane [Pandey et al., (2001a)]. The resulting material was washed and dried at room temperature and calcinated at 600 °C.

Pd-WO_3-SiO_2-PB nanocomposite was made by mixing 200 µl of PB nanosol with 10 mg powder of calcined Pd-WO_3-SiO_2 followed by sonication for 15 min. PB nanosol was made as described earlier [Pandey and Pandey, (2013b)]. The resulting Pd-WO_3-SiO_2-PB composite was allowed to dry at 65℃ for overnight.

Pd-WO_3-SiO_2-PB-HRP system was made by mixing 10 mg powder of Pd-WO_3-SiO_2-PB followed by addition of 50µl of HRP solution (10 mg/ml) made in 0.1M phosphate buffer pH,7.0. The resulting mixtures of each system were then homogenized for 5 min followed by drying.

4.2.3. Instrument

The X-ray powder diffraction patterns were obtained on Rigaku miniflex diffractometer using nickel filtered Cu Ka (l=0.15406 nm) radiation. Identification of the phase was made with the help of the JCPDS files. Transmission electron microscopy (TEM) studies were performed using Hitachi 800 and 8100 electron microscopes (Tokyo, Japan) with an acceleration voltage of 200 kV. Atomic force microscopy (AFM) image was recorded through Veeco Nanoscope IV multimode AFM (Veeco Metrology group, Santa Barbara, CA). Electrochemical measurements were performed on an electrochemical workstation CHI 660B (CH Instrument, USA) in a three-electrode cell configuration equipped with graphite paste electrode as working electrode, an Ag/AgCl reference and a platinum plate counter electrode with a working volume of 3 mL. All potentials given below were relative to the Ag/AgCl. Electrochemical characterisations (cyclic voltammetry) of Pd-WO3-SiO2 /Pure Pd electrode were conducted in 0.1 M H_2SO_4. All experiment for electrochemical analysis of AA were conducted in 0.1 M phosphate buffer solution (pH 7.0) containing 0.5 M KCl.

4.2.4. Fabrication of electrodes

The electrode body from Bioanalytical Systems West Lafayette, IN (MF 2010)) was used for the fabrication of graphite paste electrode. The well of electrode body was filled with active paste made by mixing graphite powder and Pd-WO_3-SiO_2 /Pure Pd powder using nujol. The composition of active paste was Pd-WO_3-SiO_2/Pure Pd = 1% (w/w), graphite powder = 69% (w/w) and nujol oil = 30% (w/w). And for electroanalysis of the AA the well of electrode body was filled with active paste made by mixing graphite powder and WO_3/WO_3-PB /Pd-WO_3-SiO_2 /Pd-WO_3-SiO_2-PB/Pd-WO_3-SiO_2-PB-HRP powder using nujol. The composition of active paste was WO_3/Pd-WO_3-SiO_2/Pd-WO_3-SiO_2-PB = 1% (w/w), graphite powder = 69% (w/w) and nujol oil = 30% (w/w). The mixture was homogenized in the blender and stored in a stoppard glass vial at room temperature or at 4^oC in case of enzyme electrode when not in use. The paste surface was manually smoothened on a clean paper.

4.2.5. Studies on the photometric response of aqueous WO_3, Pd-WO_3-SiO_2 and Pd-WO_3-SiO_2-PB nano suspension

The peroxidase like activity of WO_3, Pd-WO_3-SiO_2, and Pd-WO_3-SiO_2-PB nanocomposite has been studied as a function of H_2O_2 concentration. Steady-state kinetics was performed by varying the concentration of H_2O_2 (0-50 mM) at a fixed concentration of o-dianisidine. The reaction was carried out in 2 mL phosphate buffer (0.1 M, pH 7.0) and the variation of the absorbance was monitored using a spectrophotometer (Hitachi U-2900) in the time scan mode at 430 nm (ε = 11.3 $mM^{-1}cm^{-1}$). The kinetic parameters were calculated by fitting the absorbance data to the Michaelis–Menten equation as,

$$V = V_{max}\,[C]/K_m + [C]$$

Where V is the initial velocity, V_{max} is the maximal reaction velocity, C is the concentration of the substrate, and K_m is the Michaelis–Menten constant.

4.3. RESULT AND DISCUSSION

4.3.1. XRD analysis

The first stage of the investigation is to characterize the as synthesized WO_3 (a) Pd-WO_3-SiO_2 (b) and Pd-WO_3-SiO_2-PB (c) nanocomposite in order to validate the synthesis of as proposed materials shown in Figure 4.1. For this, the Pd-WO_3-SiO_2-PB was confirmed by XRD analysis. Figure 4.2 depicts the XRD patterns of Pd-WO_3-SiO_2-PB nanocomposite and shows all the characteristic peaks of WO_3, Pd and PB (17.3, 24.6, 35.2, 39.6 corresponding to 100, 110, 200, 210 crystalline plane). Inset of Figure 4.2 shows XRD pattern of the calcinated WO_3 nanoparticle at 450 $^{\circ}$C (A) and Pd-WO_3-SiO_2 nanocomposite at 600 $^{\circ}$C (B). The results of XRD pattern indicate that WO_3 nanopowder is well-crystalline and reveals diffraction peaks corresponding to monoclinic structure. The intensities and positions of the peaks are in agreement with the literature and corresponding software (JCPDS card, No. 4-0593). The broadening of diffraction peaks is a typical characteristic of nano dimensional crystals [Yin et al., (2002)]. The characteristic peaks of palladium in Pd-WO_3-SiO_2 nanocomposite are present at 40.18 and 46.68, corresponded to (111) and (110) crystalline plane. The mean crystallite sizes of WO_3 and Pd-WO_3-SiO_2 nanocomposite are found to be 52.6, 67.3 nm respectively based on Debye-Scherrer equation.

4.3.2. TEM analysis

The morphology of WO_3, Pd-WO_3-SiO_2 and Pd-WO_3-SiO_2-PB nanocomposite was analysed by transmission electron microscopy (TEM). The TEM image of WO_3 nanoparticles as shown in Figure 4.3 reveals the rods and spheroids shape nanogeometry however agglomeration of nanoparticle occurs. The Pd-WO_3-SiO_2 nanoparticles show tetragonal geometry which confirmed the role of SiO_2 in the development of particular morphology of nanomaterial and also decrease the agglomeration due to presence of SiO_2 matrix. TEM image of resulting nanocomposite material of Pd-WO_3-SiO_2 with PB shows ordered spheroid geometry that may impart large surface-to-volume ratio of

Pd-WO_3-SiO_2-PB nanocomposite. The average particle size of resulting Pd-WO_3-SiO_2-PB nanocomposite was found to be 85 nm based on imageJ software as shown in inset of Figure 4.3.

4.3.3. FTIR spectral analysis

The WO_3, Pd-WO_3-SiO_2 and Pd-WO_3-SiO_2-PB materials were further confirmed by IR spectra shown in Figure 4.4 represents the characteristics peak of crystalline WO_3 at 700, 814, 861 and 893cm^{-1}. IR spectra of Pd-WO_3-SiO_2 composite represent the peaks at 814 cm^{-1} corresponding to symmetrical stretching vibration of the SiO_2, W-O stretching in WO_3 correspond to peak at 962 cm-1 and vibration of the W=O and W-OH at 1041and 1433cm^{-1}. The Pd-WO_3-SiO_2 composite was made having similar ratio of WO_3 and SiO_2, the corresponding peaks at 962 and 1041 cm^{-1}. The Pd-WO_3-SiO_2-PB composite have all the similar paeks corresponding to Pd-WO_3-SiO_2 composite and find extra peaks at 500, 1080, 1260 and 2110 cm^{-1} corresponding to PB. The absorption at 2110 cm^{-1} attributed to the CN stretching in the formed [Fe^{II}–CN–Fe^{III}] structure. The peaks at 1649 and 3400 cm-1 correspond to bending vibration of adsorbed H_2O molecule.

Figure 4.1. Photograph of WO_3 **(a)**, Pd-WO_3-SiO_2 **(b)** and Pd-WO_3-SiO_2-PB **(c)** nanocomposite.

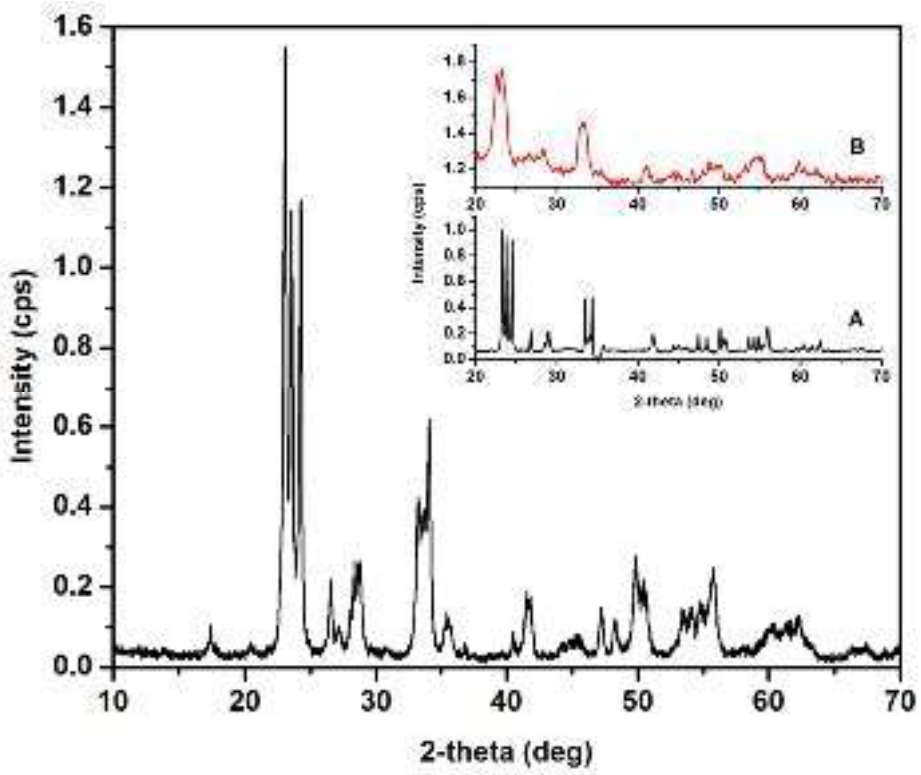

Figure 4.2. XRD patterns of Pd-WO_3-SiO_2-PB nanocomposite; inset shows the XRD pattern of calcined WO_3 at 450 ^{0}C (A) and Pd-WO_3-SiO_2 at 600 ^{0}C (B).

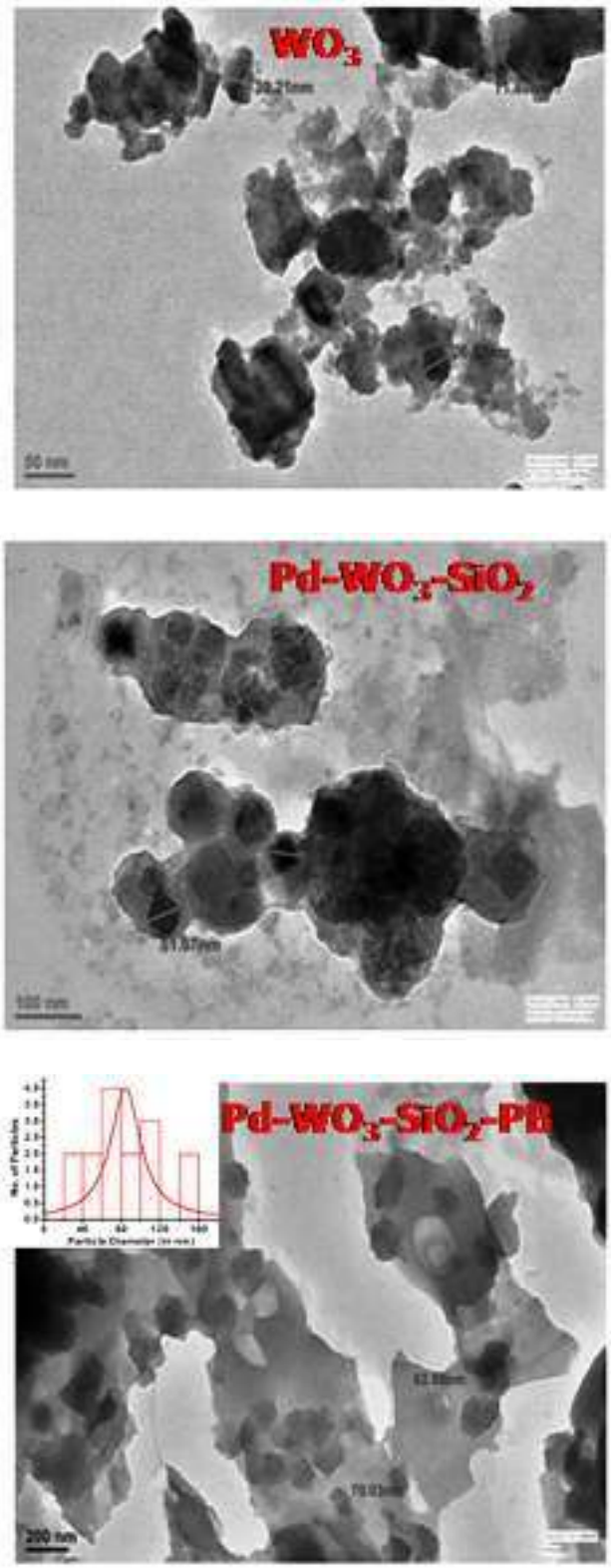

Figure 4.3. TEM image of WO_3, Pd-WO_3-SiO_2, Pd-WO_3-SiO_2-PB nanocomposite.

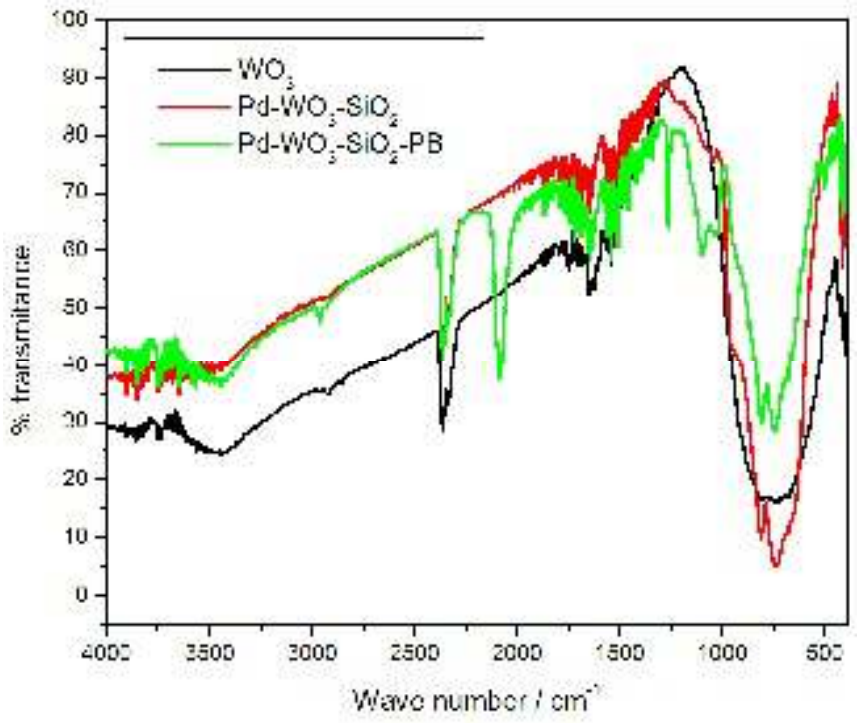

Figure 4.4. FTIR Spectra of WO_3, Pd-WO_3-SiO_2, Pd-WO_3-SiO_2-PB nanocomposite.

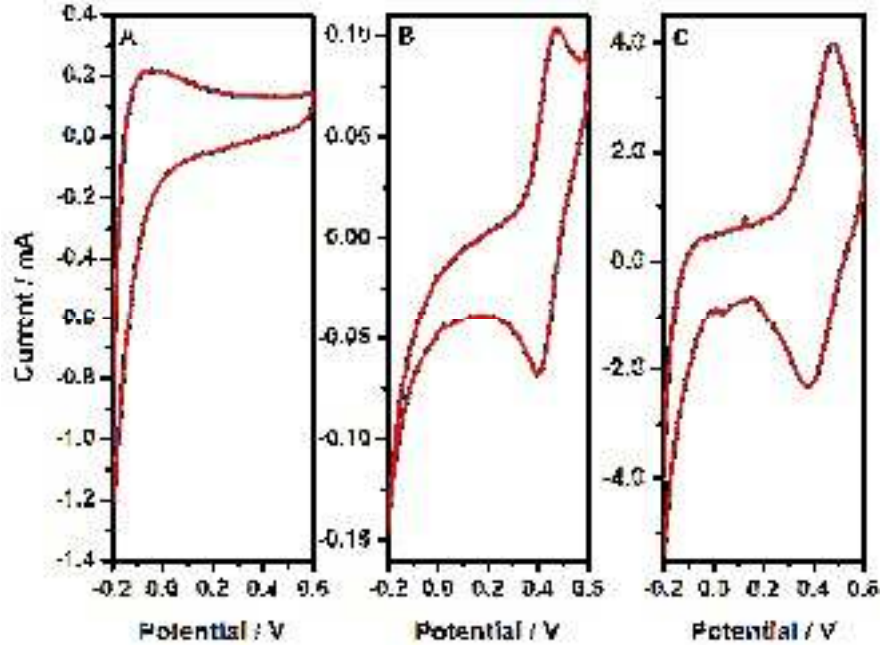

Figure 4.5. The Cyclic voltamogramme of WO_3 **(A)**, Pd-WO_3-SiO_2**(B)**, Pure Pd **(C)** modified graphite paste electrode in 1M H_2SO_4.

4.3.4. Electrochemical analysis of Pd-WO_3-SiO_2 nanocomposite

We studied the electrochemistry of WO_3, Pd-WO_3-SiO_2 and pure Pd electrodes in 1M H_2SO_4. Figure 4.5 A shows the cyclic voltammogram (CV) of WO_3 and Figure 4.5 B shows that of Pd-WO_3-SiO_2 whereas Figure 4.4 C shows the cyclic voltammogram (CV) pure Pd. In all cases CV was performed over a carbon paste electrode containing 1 % of the respective materials as modifiers. The voltammograms (Figure 4.5 C) justify that CV of pure Pd shows a well defined redox couple of oxygen adsorption (at~ 0.538 V) and stripping (at ~ 0.418 V) during anodic and cathodic scans respectively. These results are consistent with that reported for electrodeposited Pd in H_2SO_4. The CV of Pd-WO_3-SiO_2 (4.5 B) also shows redox behaviour at identical potential values as that in Figure 4.5 C but this is not as prominent as that of the former which may be due to the interaction of Pd with TiO_2 and SiO_2 followed by composite formation. However, in both the cases the redox process observed is extremely sensitive to pH of the medium and disappears at neutral or even lower acidic pH. We did not observe this redox process at pH 7 which was the working medium for the analysis of hydrogen peroxide.

4.3.5. Evaluation of the electrocatalytic performance of WO_3 and its nanocomposites

- ***Cyclic voltammetry***

The electrocatalytic performance of WO_3, Pd-WO_3-SiO_2, WO_3-PB and Pd-WO_3-SiO_2-PB is examined to understand their role on H_2O_2 sensing. HRP has also been coupled to Pd-WO_3-SiO_2-PB nanocomposite to study an increase in efficiency of electrocatalysis, of the composite material. Figure 4.6 A-E shows the cyclic voltammograms of WO_3, Pd-WO_3-SiO_2, WO_3-PB, Pd-WO_3-SiO_2-PB and HRP coupled Pd-WO_3-SiO_2-PB systems respectively in absence (1) and the presence (2) of 1 mM H_2O_2 in 0.1M phosphate buffer (pH 7.0) containing 0.5 M KCl. The occurrence of remarkable variation in cathodic peak current values on the addition of H_2O_2 justifies the electrocatalytic behaviour of WO_3, Pd-WO_3-SiO_2 and Pd-WO_3-SiO_2-PB nanocomposite. The results also

justify that Pd enhances the catalytic nature of WO_3. Since PB is known to catalyze the H_2O_2, incorporation of the same in nanocomposite significantly increases the catalytic property of the Pd-WO_3-SiO_2-PB nanocomposite. The cyclic voltammetric result of HRP-immobilized Pd-WO_3-SiO_2-PB nanocomposites modified electrode in absence (1) and the presence (2) of 1 mM H_2O_2 illustrate the reduction of H_2O_2 close to the redox potential of PB with significant increase in magnitude of cathodic current as compared to that of in absence of HRP keeping other conditions constant.

- ***Amperometry***

In order to study the quantitative determination of H_2O_2 reduction, the amperometric responses at WO_3, Pd-WO_3-SiO_2, WO_3-PB systems were recorded as shown in Figure 4.7 on the addition of varying concentrations of H_2O_2 (10 nM to 5 mM) in phosphate buffer (0.1 M, pH 7.0) at working potential of 0.2 V vs. Ag/AgCl . Figure 4.7 clearly depicted the effect of Pd and PB. The amperometric responses at Pd-WO_3-SiO_2-PB and Pd-WO_3-SiO_2-PB-HRP systems were also recorded as shown in Figure 4.8 on the addition of varying concentrations of H_2O_2 (10 nM to 5 mM) as same condition. It is clear from Figure 4.8 (curve-2) that the HRP coupled Pd-WO_3-SiO_2-PB nanocomposite shows nearly 7 fold increase in amperometric response as compared to that of Pd-WO_3-SiO_2-PB (Figure 4.8 curve-1) system, justifying the role of enzyme catalyzed reduction of H_2O_2 at 0.2V vs Ag/AgCl. H_2O_2 undergoes direct reduction at negative potential (−0.1 V vs. Ag/AgCl) over bare electrodes and the kinetics of such reduction increases on increasing the negative potential [Pandey et al., (2001c)]. On the other hand non-mediated HRP-catalyzed reduction of H_2O_2 starts at slightly positive potential (0.1 V vs. Ag/AgCl) with significant increase in sensitivity on H_2O_2 sensing as compared to that of non-enzymatic reduction of the same. Similarly, reduction of H_2O_2 in the presence of HRP along with electron-transfer relays has been recorded close to the redox potential of the mediator. [Pandey et al., (2003a); Pandey et al., (2001c)] The choice of operating potential is based on increasing the

selectivity of H_2O_2 catalysis and eliminating any contribution due to direct reduction of the same. Figure 4.9 shows the calibration curves for H_2O_2 detection on Pd-WO_3-SiO_2-PB and HRP coupled Pd-WO_3-SiO_2-PB modified electrode, showing steady state currents for both electrodes with respect to concentration. The sensitivities towards H_2O_2 for Pd-WO_3-SiO_2-PB and Pd-WO_3-SiO_2-PB-HRP were found to be 99.3 and 683.5 $\mu AmM^{-1}cm^{-2}$ respectively at applied potential of 0.2 V vs. Ag/AgCl. It should be noted that the sensitivity of H_2O_2 analysis increases on decreasing the anodic potential for electrochemical detection. Moreover, the Pd-WO_3-SiO_2-PB-HRP nanocomposite sensor exhibited a linear dependence on H_2O_2 concentration (R^2= 0.9866) with a linear range of 100 nM to 1 mM.

When HRP is coupled to composite material the sensitivity of analysis is increased. Such enhancement in sensitivity is a joint contribution of matrix materials justifying a better system of enzyme immobilization and their role in biocatalysis. The interaction of HRP with this nanocomposite is based on the electrostatic interaction between negatively charged WO_3 nanomaterial (isoelectric point (IEP), ~0.5) and positively charged HRP (IEP, ~8.9) [Deng, Z. et al., (2009)].

- ***Interference study***

The detection of H_2O_2 has been performed in the presence of common interfering species like ascorbic acid (AA), uric acid and acetaminophen, and found that its overall interference effect is negligible except to that of ascorbic acid (AA). AA undergoes electrochemical oxidation and achieved a 40% response compared to H_2O_2 under similar conditions. However, it should be noted that AA has a concentration in the blood of around 25-100 μM with a maximum value of 200 μM. Therefore, its overall interference effect is negligible.

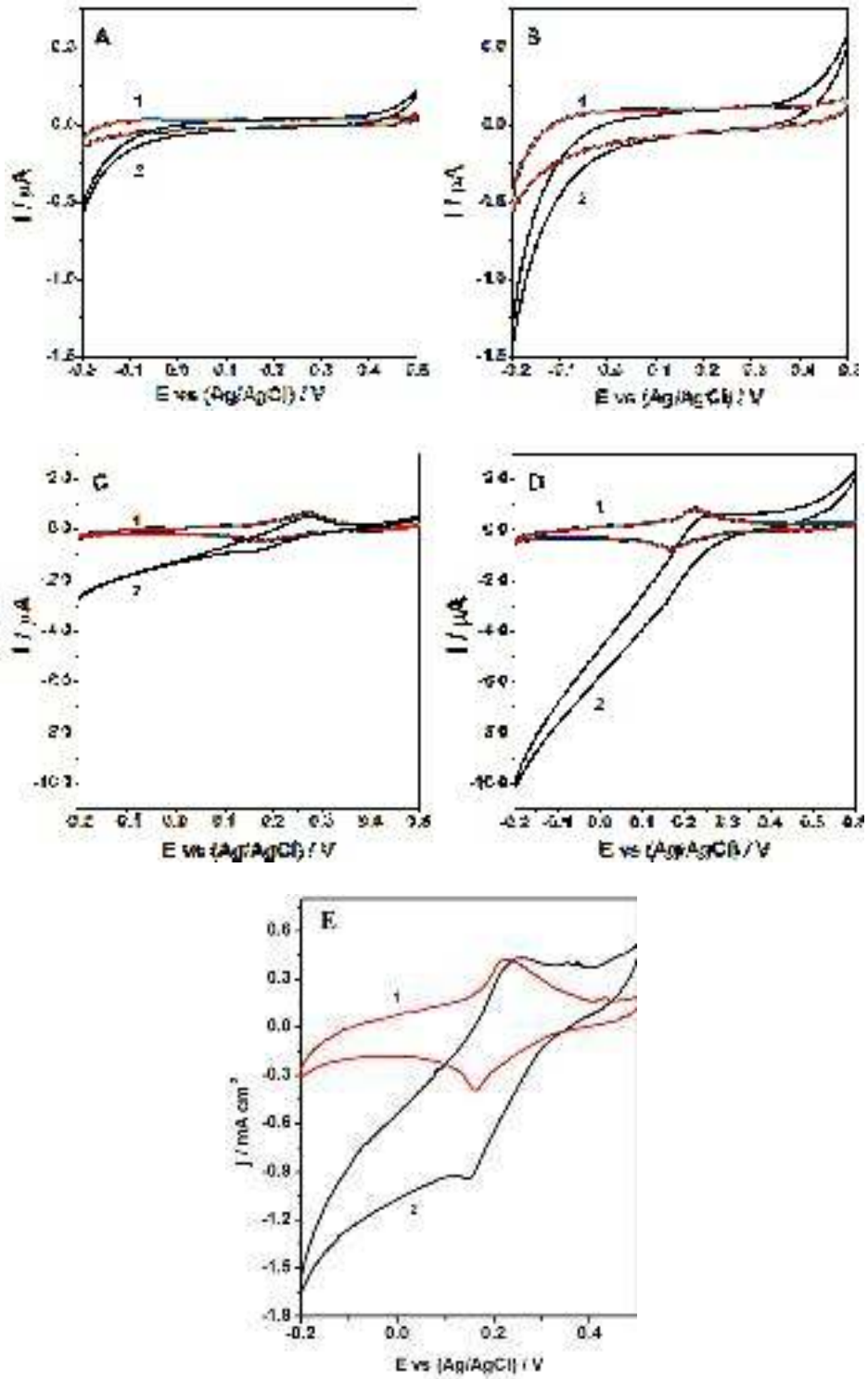

Figure 4.6. The Cyclic voltamogramme of WO_3 **(A)**, Pd-WO_3-SiO_2**(B)**, WO_3-PB **(C)**, Pd-WO_3-SiO_2-PB **(D)** and HRP coupled Pd-WO_3-SiO_2-PB **(E)** modified graphite paste electrode in absence (1) and the presence (2) of 1 mM H_2O_2 in phospahate buffer (0.1M, pH 7.0) containing 0.5 M KCl.

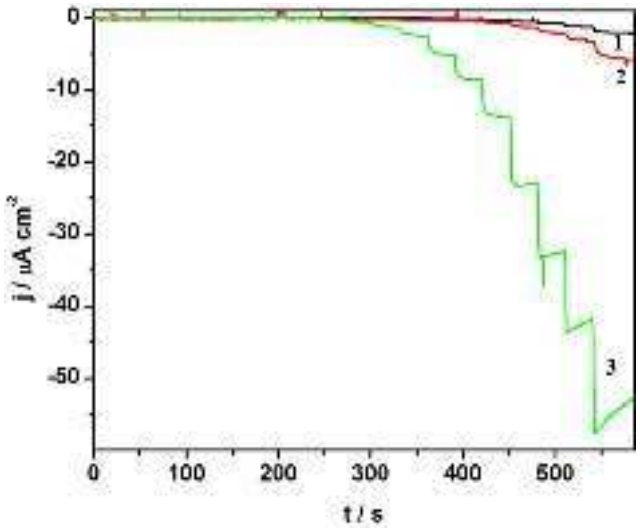

Figure 4.7. Typical amperometric responses of the WO_3 (1), Pd-WO_3-SiO_2 (2) and WO3-PB (3) modified graphite paste electrode on the addition of varying concentrations (10 nM to 5 mM) of H_2O_2 in 0.1 M phosphate buffer, pH 7.0 at 25 ^{0}C at 0.2 V vs Ag/AgCl.

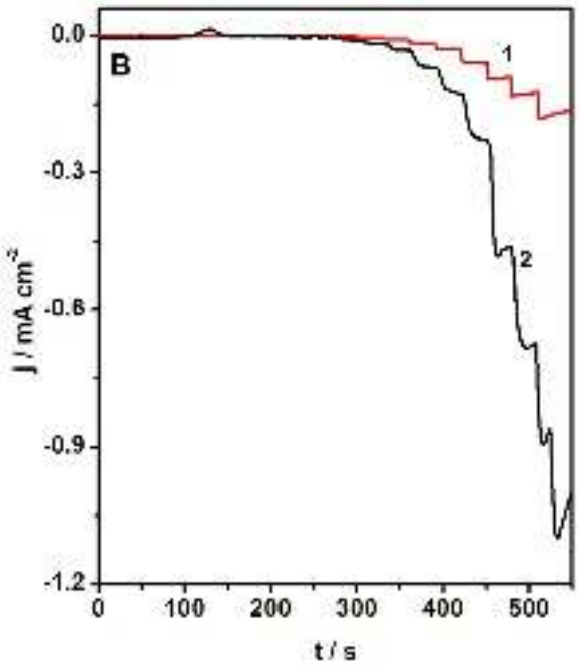

Figure 4.8. Typical amperometric responses of the Pd-WO_3-SiO_2-PB (1) and Pd-WO_3-SiO_2-PB-HRP (2) modified graphite paste electrode on the addition of varying concentrations (10 nM to 5 mM) of H_2O_2 in 0.1 M phosphate buffer, pH 7.0 at 25 ^{0}C at 0.2 V vs Ag/AgCl.

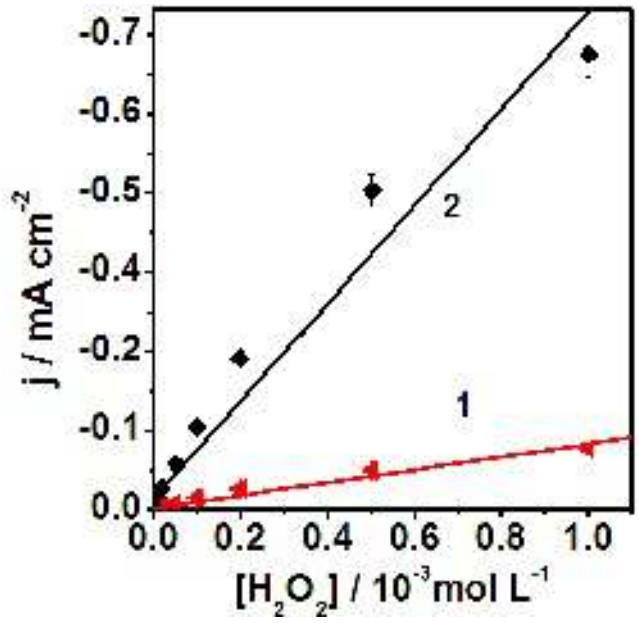

Figure 4.9. Calibration curve for H_2O_2 analysis over Pd-WO_3-SiO_2-PB (1), and Pd-WO_3-SiO_2-PB-HRP (2) modified graphite paste electrode.

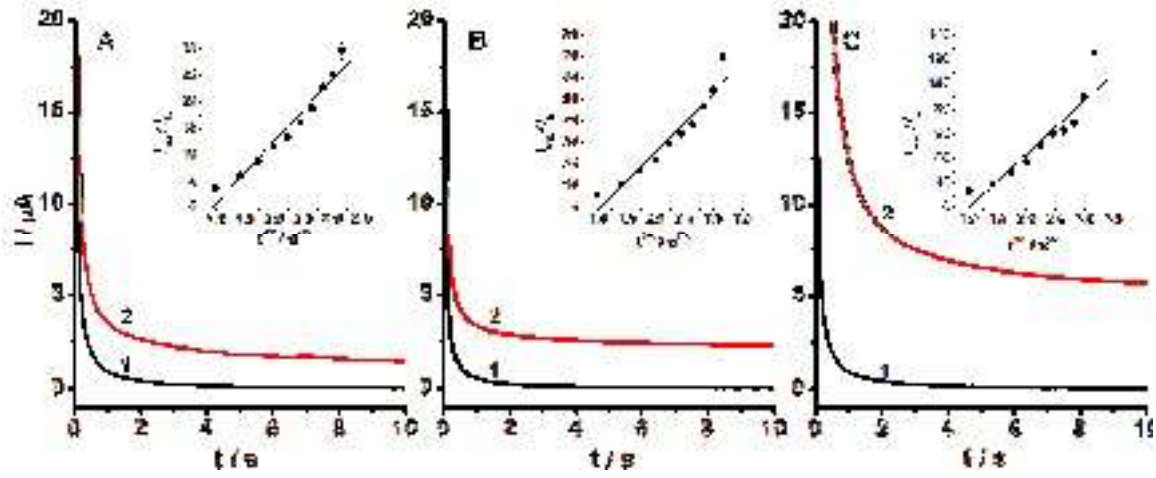

Figure 4.10. The chronoamperograms for the WO_3 **(A)**, Pd-WO_3-SiO_2 **(B)** and Pd-WO_3-SiO_2-PB **(C)** modified electrodes in absence (1) and the presence (2) of 1 mM of H_2O_2 by setting the step potential at 0.2 V vs. Ag/AgCl for subsequent evaluation of I_{cat} and $I_{L.}$ Inset: Corresponding plots of I_{cat}/I_L vs. $t^{1/2}$, supporting electrolyte 0.1 M phosphate buffer (pH, 7.0) containing 0.5 M KCl.

- ***Chronoamperometry***

In order to have further insight on the catalytic property of as synthesized materials chronoamperometry was also conducted for the evaluation of the catalytic rate constant ($k_{cat.}$) [Galus et al., (1976)]. Figure 4.10 shows the chronoamperograms for the WO_3 (A), Pd-WO_3-SiO_2 (B) and Pd-WO_3-SiO_2-PB (C) modified electrodes in absence (1) and the presence (2) of 1 mM of H_2O_2 by setting the step potential at 0.2 V vs. Ag/AgCl for subsequent evaluation of I_{cat} and $I_{L,}$ where I_{cat} and I_L represents the currents of the modified electrode in the presence and absence of H_2O_2 respectively. The plot of I_{cat}/I_L vs. $t_{1/2}$ is shown in insets of Figure 4.9 A, B and C for WO_3, Pd-WO_3-SiO_2 and Pd-WO_3-SiO_2-PB modified electrodes respectively. Over a limited time frame, the values of I_{cat}/I_L were linearly dependent on $t_{1/2}$, and from its slope k_{cat} was calculated. The values obtained were 7.34×10^3, 3.7×10^4 and 7.5×10^4 M^{-1} s^{-1} for WO_3, Pd-WO_3-SiO_2 and Pd-WO_3-SiO_2-PB system, respectively and again justify an increased catalytic efficiency of Pd-WO_3-SiO_2-PB system toward H_2O_2 reduction. The enhanced value of catalytic rate constant of present modified system shows its superiority over other modified electrodes for H_2O_2 analysis.

- ***Stability and Reproducibility***

The storage stability of the sensor was evaluated over a period of 3 months by storing the electrode in phosphate buffer (0.01 M, pH 7.0) at room temperature. Decreases of 6 to 8 % were observed in amperometric responses of the Pd-WO_3-SiO_2-PB modified electrode after storing. The stability of the same electrode was examined by cyclic voltammetry. Investigation indicated that the peak current and peak potential of the Pd-WO_3-SiO_2-PB modified electrode have remained nearly unchanged, and the amount of degradation after 50 cycles with scan rate of $20mVs^{-1}$ was less than 5 % using same batch of Pd-WO_3-SiO_2-PB modified electrode. The relative standard deviation (RSD) of the current response to 1 mM H_2O_2 at 0.2V vs Ag/AgCl is found to be 3.5 % for 16

successive measurements. Thus, it can be said that Pd-WO_3-SiO_2-PB modified electrode exhibits good stability and reproducibility for H_2O_2 detection.

4.3.6. WO_3 and its nanocomposite as peroxidase mimetic

HRP-H_2O_2-color substrate systems are typically employed for routine applications in ELISA kits and other bioassays. The catalytic mechanism involves the enzyme catalysis of the two electron reduction of H_2O_2 to H_2O to form an intermediate complex; the color substrate binds to the complex by a nucleophilic attack, thus allowing the oxidation reaction to occur with a color change. The activity of HRP in such kits remains in question as HRP is not sufficiently stable for practical applications. Accordingly, the requirement for an HRP-mimetic has been an important area of research. During the last few years, nanomaterials have shown potential peroxidase like activity and have revealed their use as a peroxidase replacement. Accordingly, there still exists a need for efficient nanomaterials having equivalent or better kinetic data than that of peroxidase. Since, WO_3, Pd-WO_3-SiO_2 and Pd-WO_3-SiO_2-PB nanocomposite has sufficient stability; an aqueous dispersion of the same may be a potential peroxidase mimetic candidate. To characterize the peroxidase like activity of the WO_3, we have done the experiments using three peroxidase substrates o-dianisidine, pyrogallol (Py) and phenol. Figure 4.11 shows that the WO_3 suspension not only catalyzed oxidation of o-dianisidine producing a orange brown color (i), but also pyrogallol to give an yellow color (ii) and phenol to give a dark brown color precipitate (iii).

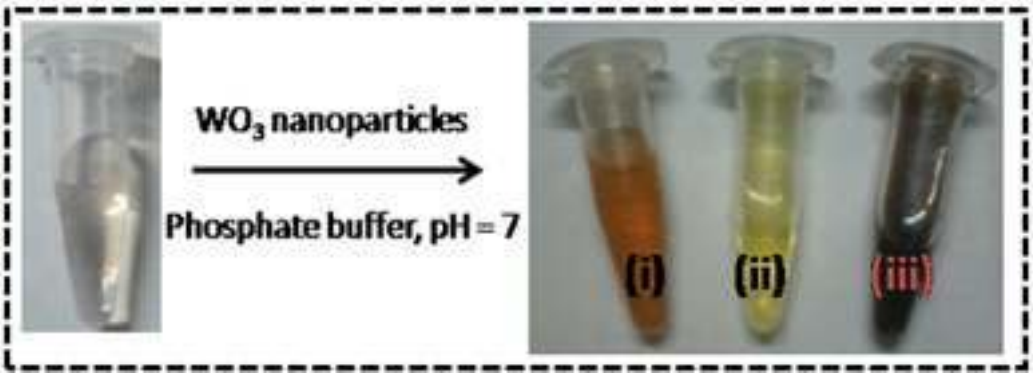

Figure 4.11. Photograph showing the production of coloured product upon the addition of WO_3 nanosuspension to: **(i)** o -dianisidine, **(ii)** pyrogallol, and **(iii)** phenol at pH 7.0.

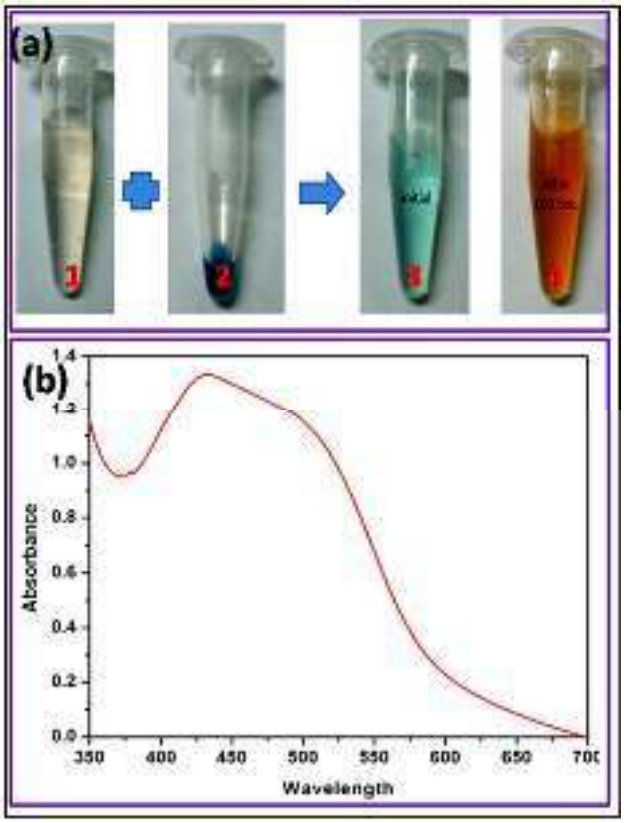

Figure 4.12. (a) Photographs showing the production of coloured product upon the addition of Pd-WO_3-SiO_2-PB nanosuspension to o–dianisidine in phosphate buffer at pH 7.0. **(b)** A simple absorbance spectra corresponding to o-dianisidine oxidation product.

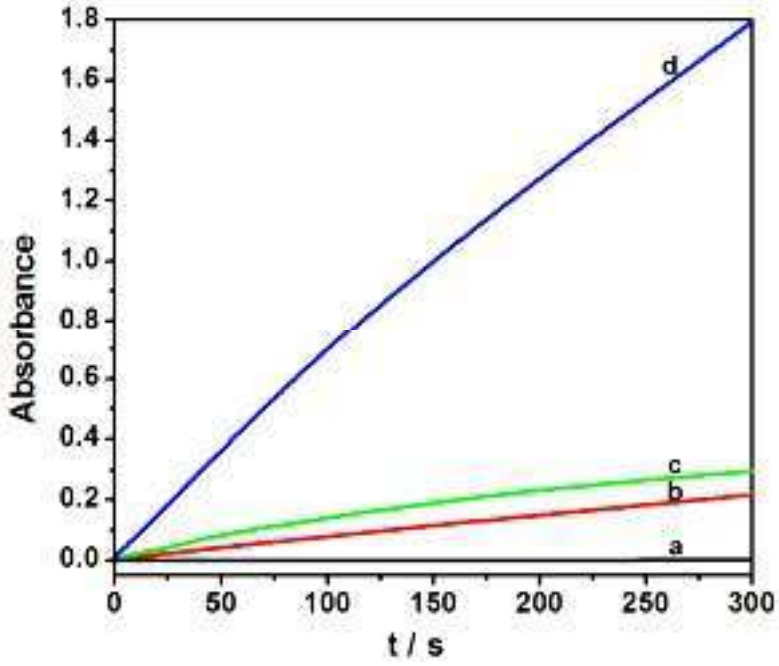

Figure 4.13. Time dependent absorbance evaluation at 430 nm corresponding to o-dianisidine oxidation product as; (a) without catalyst, (b) WO_3, (c) Pd-WO_3-SiO_2, and (d) Pd-WO_3-SiO_2-PB.

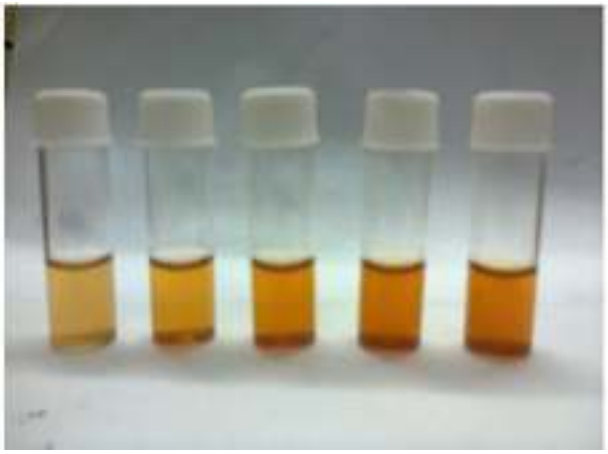

Figure 4.14. Photograph showing the production of coloured product upon the addition of varying concentration of H_2O_2.

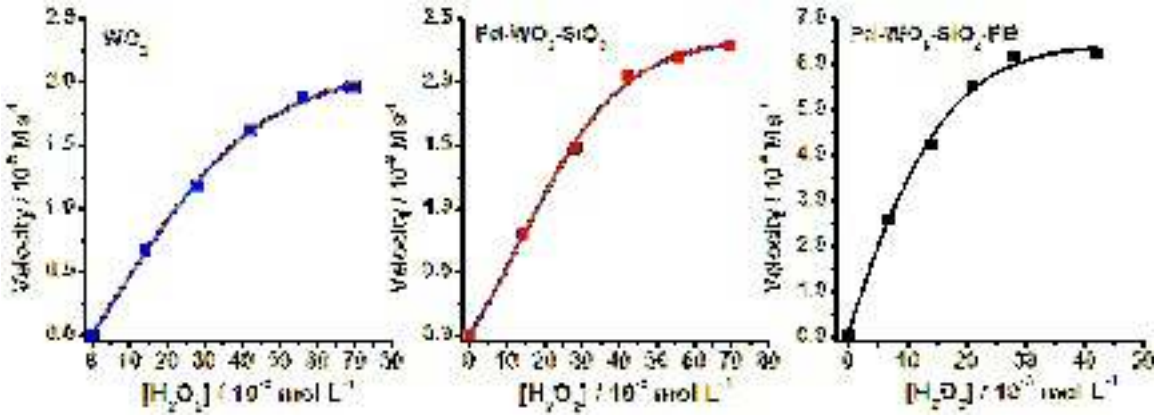

Figure 4.15. The steady state kinetic assay of WO_3, Pd-WO_3-SiO_2 and Pd-WO_3-SiO_2-PB nanosuspension with H_2O_2 as substrate.

4.3.7. Evaluation of peroxidase like activity of WO_3 and its nanocomposite: application in H_2O_2 detection

Oxidation of peroxidase substrate o-dianisidine

Recently, it is reported that many nanomaterials, such as metal oxide, noble metals nanoparticles, metal hexacyanoferrate and their composites possess intrinsic peroxidase like activity and have revealed their use as peroxidase replacement for health and health care advances [André et al., (2011); Asati et al., (2009); Guo, Yujing et al., (2011); Jv et al., (2010); Lin, Youhui et al., (2013); Zhang, Xiao-Qing et al., (2010)]. The reduction of H_2O_2 with a PBNPs based system has been extensively studied in many cases due to the analogous behavior of PB to artificial peroxidase. During recent years it has been also reported that PBNPs and its analogues possess intrinsic peroxidase like activity and used for detection of H_2O_2 [Karyakin et al., (2000); Moscone et al., (2001)]. However the peroxidase mimetic property of WO_3 nanoparticle has not been reported so far. Accordingly, attempt has been made to evaluate the peroxidase mimetic ability of as-synthesized WO_3, Pd-WO_3-SiO_2 and Pd-WO_3-SiO_2-PB nanocomposite towards the oxidation of o-dianisidine by H_2O_2. The basic principle associated to this photometric response is shown as equation-1:

H_2O_2 + o-dianisidine $_{(reduced)}$ $\xrightarrow{Catalyst}$ o-dianisidine $_{(oxidised)}$ + H_2O…….(1)

The catalytic mechanism involves the enzyme like catalysis of the two electron reduction of H_2O_2 to H_2O to form an intermediate complex and the color substrate binds to the complex by a nucleophilic attack, thus allowing the oxidation reaction to occur with a color change. The response is measured by monitoring the absorbance at 430 nm of the oxidized colour product, as a result of catalyzed reaction. The reaction mixture consists of 2.0 ml of phosphate buffer (0.1 M, containing 0.5 M KCl, pH 7.0), 25 µl H_2O_2 (30%), 25 µl of 20 mM o-dianisidine. The 25 µl aqueous suspensions of WO_3, Pd-WO_3-SiO_2 and Pd-WO_3-SiO_2-PB (5 mg/ml) are used as catalyst to carry out the reaction process. Figure 4.12 photograph (a) shows the production of coloured product upon the addition of Pd-WO_3-SiO_2-PB nanosuspension to o–dianisidine in phosphate buffer at pH 7.0 and a simple absorbance spectra (b) corresponding to o-dianisidine oxidation product. In order to analyze the kinetic activity of as synthesized nanomaterials, the time dependent absorbance was shown in Figure 4.13 recorded at 430 nm as corresponding to o-dianisidine oxidation product as; (a) without catalyst, (b) WO_3, (c) Pd-WO_3-SiO_2, and (d) Pd-WO_3-SiO_2-PB reveals the effect of Pd and PBNPs. A photograph shown in Figure 4.14 represent the production of coloured product with increases the colour intensity upon the addition of increasing the concentration of H_2O_2.

Figure 4.15 shows the steady state kinetic assay for WO_3, Pd-WO_3-SiO_2 and Pd-WO_3-SiO_2-PB composite with H_2O_2 as substrate. The Michaelis constant (K_m) of WO_3, Pd-WO_3-SiO_2, and Pd-WO_3-SiO_2-PB nanocomposite is calculated to be 23, 19.5, 8.1 mM, respectively. The results justify an increase in peroxidise mimetic behaviour in the order of WO_3 < Pd-WO_3-SiO_2 < Pd-WO_3-SiO_2-PB. The apparent K_m value of aqueous nanosuspension was compared with HRP recorded under existing experimental conditions, which confirmed that aqueous suspension of Pd-WO_3-SiO_2-PB nanocomposite shows significantly better practical usability due to relatively longer stability of the nanocomposite as compared to that of HRP. The apparent K_m value of the Pd-

WO_3-SiO_2-PB nano dispersion with H_2O_2 as the substrate was found to be 8.1 mM whereas it was 3.7 mM for HRP [Gao, Lizeng et al., (2007)]

4.4. CONCLUSION

The synthesis of WO_3, Pd-WO_3-SiO_2 and Pd-WO_3-SiO_2-PB nanocomposite reported in this chapter. The resulting nanocomposite shows spheroids morphology with average particle size of 85 nm justifying the nanogeometry of nanocomposite. The X-ray diffraction pattern resembles the characteristic of WO_3, Pd and PB in the resulting nanocomposite material. The characteristic peaks of WO_3, Pd and PB are shown in FTIR spectra further validate the composite material. A redox couple of oxygen adsorption and stripping was measured in the electroanalysis of Pd-WO_3-SiO_2 composite material also justified the presence of Pd. Pd-WO_3-SiO_2-PB nanocomposite was further coupled with HRP for enhancing the selectivity and sensitivity of the H_2O_2 reduction. The electrocatalytic activity of WO_3, Pd-WO_3-SiO_2, WO_3-PB, Pd-WO_3-SiO_2-PB and HRP coupled Pd-WO_3-SiO_2-PB was analyzed by cyclic voltammetry and amperometry for the reduction of the biologically significant analyte H_2O_2. The cyclic voltammetry results justifying the role of Pd, PB and HPR for significant increase in magnitude of cathodic current of HRP coupled Pd-WO_3-SiO_2-PB as compared to that of WO_3, Pd-WO_3-SiO_2, WO_3-PB and Pd-WO_3-SiO_2-PB. The Pd-WO_3-SiO_2-PB modified electrode exhibit a good sensitivity towards H_2O_2 to the order of 99.3 $\mu AmM^{-1}cm^{-2}$ in absence and 683.5$\mu AmM^{-1}cm^{-2}$ in the presence of HRP with a linear detection range of 100 nM to 1 mM at working potential of 0.2V vs Ag/AgCl. The chronoamperometry results demonstrate the electrocatalytic rate constant for the H_2O_2 is found to the order of WO_3 < Pd-WO_3-SiO_2 < Pd-WO_3-SiO_2-PB. These findings justify the role of WO_3 and Pd-WO_3-SiO_2 nanostructure material for improving the catalytic character of PBNPs.

Herein, we also investigated that WO_3, Pd-WO_3-SiO_2 and Pd-WO_3-SiO_2-PB nanocomposite possess intrinsic peroxidase like activity capable of catalyzing the oxidation of typical substrate o-dianisidine, phenol and Py by H_2O_2. WO_3 and Pd-WO_3-SiO_2 nanocomposite material enhances the excellent

peroxidase mimetic of PBNPs for the reduction of the biologically significant analyte H_2O_2. The Michaelis constant (Km) of these materials are found in the order of Pd-WO_3-SiO_2-PB > Pd-WO_3-SiO_2 > WO_3. These results justify the role of WO_3 and Pd-WO_3-SiO_2 nanostructure material for improving the catalytic character of PBNPs.